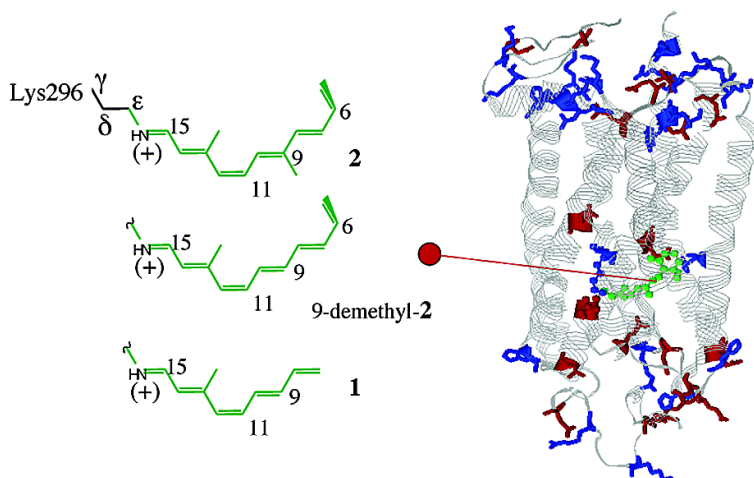


Probing the Rhodopsin Cavity with Reduced Retinal Models at the CASPT2//CASSCF/AMBER Level of Theory

Nicolas Ferr, and Massimo Olivucci

J. Am. Chem. Soc., **2003**, 125 (23), 6868-6869 • DOI: 10.1021/ja035087d • Publication Date (Web): 16 May 2003

Downloaded from <http://pubs.acs.org> on March 29, 2009



More About This Article

Additional resources and features associated with this article are available within the HTML version:

- Supporting Information
- Links to the 20 articles that cite this article, as of the time of this article download
- Access to high resolution figures
- Links to articles and content related to this article
- Copyright permission to reproduce figures and/or text from this article

[View the Full Text HTML](#)

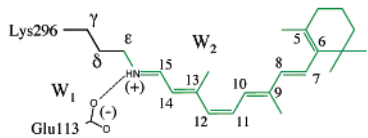
Probing the Rhodopsin Cavity with Reduced Retinal Models at the CASPT2//CASSCF/AMBER Level of Theory

Nicolas Ferré† and Massimo Olivucci*†,‡

Dipartimento di Chimica, Università di Siena, via Aldo Moro I-53100 Siena, Italy, and Centro per lo Studio dei Sistemi Complessi, Via Tommaso Pendola 37, Siena I-53100 Italy

Received March 10, 2003; E-mail: olivucci@unisi.it

The visual pigment rhodopsin^{1,2} (Rh) is a G-protein-coupled receptor containing an 11-*cis* retinal chromophore (PSB11) bounded to a lysine residue (Lys296) via a protonated Schiff base linkage (see green substructure below). While the biological activity of Rh



is triggered by the light-induced isomerization of PSB11, this reaction owes its efficiency (e.g. short time scale and quantum yields) to the protein cavity.¹ Accordingly, the investigation of the environment-dependent properties of PSB11 is a prerequisite for understanding Rh “catalysis”. The equilibrium geometry and absorption maximum (λ_{\max}) are indicators of the environment effect. In fact, while the geometry of PSB11 is nearly planar in a crystal,³ in bovine Rh it has a helical conformation.⁴ Similarly, the 445 nm λ_{\max} observed for PSB11 in methanol⁵ is red-shifted to 498 nm in Rh.^{1,2}

Recent studies⁶ on a (vacuum) five double-bond reduced model of the PSB11 cation suggest that the level of theory required for a correct description of its geometrical and electronic structure must include the treatment of electron dynamic correlation. In particular, the use of an ab initio CASPT2//CASSCF/6-31G* strategy (i.e., geometry optimization at the CASSCF level and energy evaluation at the CASPT2 level) yields reasonable values for the backbone geometry, λ_{\max} , and change in dipole moment ($\Delta\mu$) when compared with the PSB11 solution data. Here we show that the same strategy can be successfully used within a quantum mechanics/molecular mechanics (QM/MM) scheme allowing for CASPT2//CASSCF geometry optimization and excited state (e.g. S_1 and S_2) property evaluation in proteins. Two Rh models (**Rh-1** and **Rh-2**) that only differ in the PSB11 model (**1** and **2** in Figure 1) are investigated. It is shown that **Rh-2** features a chromophore equilibrium structure with the correct helicity and a λ_{\max} only 54 nm blue-shifted from the observed value.

While a number of QM/MM studies have been reported⁷ for rhodopsin proteins, only few employed ab initio QM. Yamada et al.⁸ used an RHF/6-31G/AMBER scheme to investigate the ground state (S_0) stability of PSB11 in Rh. Hayashi et al.⁹ reported a CASSCF//HF/DZV/AMBER computation of the λ_{\max} of the related pigment bacteriorhodopsin (bR). While these authors correctly predict the λ_{\max} changes among different bR photocycle intermediates, the λ_{\max} absolute values were strongly blue-shifted.

Our QM/MM scheme is fully described in the Supporting Information. Briefly, the method is based on a hydrogen link-atom

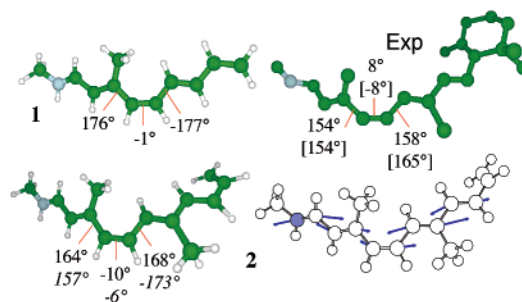


Figure 1. CASSCF optimized structures for **Rh-1**, **Rh-2** (only the corresponding chromophores **1** and **2** are displayed), and **9-demethyl-Rh-2** (italics) compared to the crystallographic⁴ and NMR¹⁴ (brackets) structure **Exp**. The arrows represent the S_1 forces in **Rh-2**.

scheme¹⁰ with the frontier placed at the C_5-C_6 bond of the Lys296 side chain (see structure above). The QM calculations are based on a CASSCF/6-31G* level. The active space comprises the full π -system of **1** and **2**. The MM (we use the AMBER force field) and QM segments interact in the following way: (i) the QM electrons and the full set of MM point charges interact via the one-electron operator, (ii) stretching, bending, and torsional¹¹ potentials involving at least one MM atom are described by the MM potential, (iii) QM and MM atom pairs separated by more than two bonds interact via either standard or re-parametrized¹¹ van der Waals potentials. CASSCF/6-31G*/AMBER geometry optimization is carried out with the GAUSSIAN98¹² and TINKER¹³ programs.

The protein framework used in the computation (see the Supporting Information for details) is derived from monomer A deposited in the PDB archive as file 1HZX.⁴ With the exception of the Glu113 counterion (forming a salt bridge with NH(+)), the Rh cavity is set neutral consistently with the experiment.¹⁵ While the protein is kept frozen during the optimization, the Lys296 side chain, the position/orientation of two TIP3P water molecules (W_1 and W_2 in the structure above), and the chromophore are relaxed.¹⁶ In the optimization of **Rh-2** the terminal $C_5-C_6-C_7-C_8$ dihedral angle of **2** is kept frozen at the crystallographic value (ca. -60°) to mimic the presence of the β -ionone ring located in a tight hydrophobic pocket (the C_7-C_8 moiety remains in the pocket during the optimization). At the equilibrium geometry, a three-root state average CASPT2 computation is carried out using the MOLCAS-5¹⁷ program to evaluate the λ_{\max} and the oscillator strength (f) of the $S_0 \rightarrow S_1$ and $S_0 \rightarrow S_2$ transitions. The AMBER charges account for S_0 polarization effects in a mean-field way.¹⁸ The same charges are used for the excited state computations with no ad hoc dielectric constant.

Similar to its N-demethyl analogue,⁶ the vacuum S_0 equilibrium geometry of **1** is planar. Insertion of this chromophore in the chiral cavity of Rh is expected to lead to a twisted conformation. Inspection of the **Rh-1** optimized structure (see Figure 1) shows

† Università di Siena.

‡ Studio dei Sistemi Complessi.

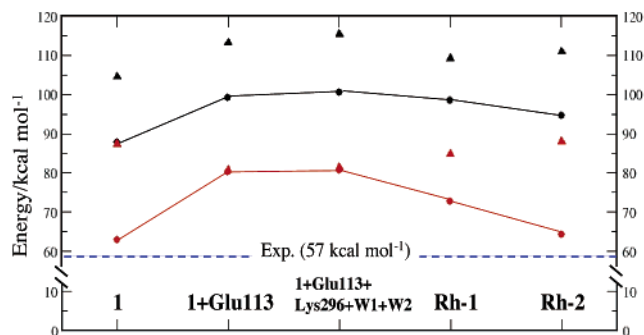


Figure 2. $S_0 \rightarrow S_1$ (circles) and $S_0 \rightarrow S_2$ (triangles) excitation energies computed at the CASSCF (black) and CASPT2 (red) QM levels.

Table 1. Oscillator Strength

structure	$S_0 \rightarrow S_1$	$S_0 \rightarrow S_2$
1	0.77	0.32
1+Glu113	0.13	0.86
Rh-1	0.39	0.68
Rh-2	0.46	0.45

that this is not the case. Chromophore **1** fits loosely in the protein cavity and the steric/electrostatic interactions do not significantly perturb its π -skeleton. In contrast, the **Rh-2** optimized structure shows a chromophore conformation remarkably close to the one observed for PSB11 in Rh.^{4,14} (This structure is similar to the one obtained by Sugihara et al.¹⁹ via DFTB computations on a reduced Rh model comprising the entire PSB11 unit.) In fact, the **Rh-2** chromophore has a spiral-like structure with the correct negative (counterclockwise) helicity. The degree of helicity depends on both the PSB11 model and the methyl substituents as **9-demethyl-Rh-2** demonstrates (see data in Figure 1).

It is established⁶ that, in vacuo, the S_1 state of a PSB11 model has a dominant hole-pair (ionic) character. Indeed, upon $S_0 \rightarrow S_1$ excitation, ca. half of the positive charge initially located on the $-\text{N}=\text{C}_{15}-$ moiety moves away along the π -skeleton leading to large values of $\Delta\mu$ and f . In contrast, the S_2 state has a dot-dot (covalent) character, the charge remains on $-\text{N}=\text{C}_{15}-$ leading to low $\Delta\mu$ and f values for the $S_0 \rightarrow S_2$ transition. In Figure 2 we show that, in vacuo, **1** (taken with the **Rh-1** optimized geometry of Figure 1) has a CASPT2 $S_0 \rightarrow S_1$ excitation energy corresponding to a 454 nm λ_{max} . As expected for an isolated PSB11 model, the magnitude of f^{20} in Table 1 indicates that the S_1 state has a larger ionic character with respect to S_2 .

When we add to **1** the counterion with its **Rh-1** geometry (**1+Glu113**), the S_1-S_0 energy gap increases, leading to a strongly blue-shifted λ_{max} . Further, the small f value indicates that the S_1 state has now a covalent character. This effect is rationalized by the fact that Glu113 stabilizes preferentially the S_0 and S_2 states where the positive charge is located at $-\text{N}=\text{C}_{15}-$, yielding a larger S_1-S_0 gap and a smaller (nearly degenerate at the CASPT2 level) S_2-S_1 gap. These effects are independent of the presence of the water molecules and Lys296 side chain (**1+Glu113+Lys296+W1+W2**). In Figure 2 we show that, at all levels, the neutral protein cavity of **Rh-1** counterbalances the Glu113 effect by decreasing the S_1-S_0 gap. A related effect has been seen by Vreven et al.²¹ in a TD-B3LYP//B3LYP/6-31G*/AMBER ONIOM computation on bR. The recovery is more complete at the CASPT2 level, suggesting that dynamic correlation is more important in the protein than in vacuo. Consistently f increases for the $S_0 \rightarrow S_1$ and decreases for the $S_0 \rightarrow S_2$ transitions with the S_1 state regaining ionic character. The prediction of the $S_0 \rightarrow S_1$ excitation energy

improves in **Rh-2** where one has the full PSB11 π -system. The computed λ_{max} is 446 nm, yielding a 52 nm (ca. 7 kcal mol⁻¹) error with respect to the experiment. This prediction will improve in full Rh where, in contrast to **Rh-2**, the β -ionone ring is not missing. In fact, simple inductive-effect considerations indicate that λ_{max} will be red-shifted by the preferential stabilization of S_1 where the positive charge is located closer to the ring alkyl groups. To characterize the initial motion of PSB11 out the vertical excitation region, we have computed the QM/MM S_1 forces in **Rh-2**. The components displayed in Figure 1 show that despite the protein chiral environment the force prompts a double-bond expansion single-bond contraction along the entire chromophore backbone with the only exception of the weakly conjugating $\text{C}_5-\text{C}_6-\text{C}_7$ fragment. This result is consistent with the previously proposed^{6,22} two-mode (first stretching then torsion) Rh isomerization coordinate. In conclusion, we have shown that a CASPT2//CASSCF/6-31G*/AMBER can be used to study the structure and spectroscopy of Rh opening the way to the investigation of the early S_1 transient species involved in the vision process.

Acknowledgment. Funds have been provided by the Università di Siena (Progetto di Ateneo 02/04) and HFSP (RG 0229/2000-M). N.F. is grateful for the EU Grant HPMF-CT-2001-01769. We thank CINECA for granted calculation time.

Supporting Information Available: Details of the QM/MM scheme and protein model. Coordinates of all optimized structures. S_1 forces of **2** in **Rh-2**. Tables of energies, charge distribution, $\Delta\mu$, and f . This material is available free of charge via the Internet at <http://pubs.acs.org>.

References

- (1) Mathies, R. A.; Lugtenburg, J. In *Handbook of Biological Physics*; Stavenga, D. G., de Grip, W. J., Pugh, E. N., Eds.; Elsevier Science B. V.: 2000; Vol. 3.
- (2) Kandori, H.; Schichida, Y.; Yoshisawa, T. *Biochemistry (Moscow)* **2001**, *66*, 1197–1209.
- (3) Santarsiero, B. D.; James, M. N. G. *J. Am. Chem. Soc.* **1990**, *112*, 9416–9418.
- (4) Teller, D. C.; Okada, T.; Behnke, C. A.; Palczewski, K.; Stenkamp, R. E. *Biochemistry* **2001**, *40*, 7761–7772.
- (5) Freedman, K. A.; Becker, R. S. *J. Am. Chem. Soc.* **1986**, *108*, 1245–1251.
- (6) Gonzalez-Luque, R.; Garavelli, M.; Bernardi, F.; Merchan, M.; Robb, M. A.; Olivucci, M. *Proc. Natl. Acad. Sci. U.S.A.* **2000**, *97*, 9379–9384.
- (7) Rajamani, R.; Gao, J. *J. Comput. Chem.* **2002**, *23*, 96–105.
- (8) Yamada, A.; Kakitani, T.; Yamamoto, S.; Yamato, T. *Chem. Phys. Lett.* **2002**, *366*, 670–675.
- (9) Hayashi, S.; Tajkhorshid, E.; Schulten, K. *Biophys. J.* **2002**, *83*, 1281–1297.
- (10) Singh, U. C.; Kollman, P. A. *J. Comput. Chem.* **1986**, *7*, 718–730.
- (11) One torsion ($\text{C}_{15}-\text{N}-\text{C}_6-\text{C}_5$) and the van der Waals forces of the PSB11 model (except NH+) have been re-parametrized to reproduce the CASSCF torsional energy profiles of a model of the frontier. See Supporting Information.
- (12) Frisch, et al. Revision A.7 ed.; Gaussian, Inc.: Pittsburgh, PA, 1998.
- (13) Ponder, J. W.; Richards, F. M. *J. Comput. Chem.* **1987**, *8*, 1016–1024.
- (14) Verdegem, P. J. E.; Bovee-Geurts, P. H. M.; De-Grip, W. J.; Lugtenburg, J.; De-Groot, H. J. M. *Biochemistry* **1999**, *38*, 11316–11324.
- (15) Fahmy, K.; Jager, F.; Beck, M.; Zvyaga, T. A.; Sakmar, T. P.; Siebert, F. *Proc. Natl. Acad. Sci. U.S.A.* **1993**, *90*, 10206–10210.
- (16) The optimized W_1 position differs from the one proposed by Okada et al. See the Supporting Information.
- (17) Andersson, K. et al. Version 5 ed.; University of Lund: Lund, Sweden, 2002.
- (18) Besler, B.; Merz, K.; Kollman, P. *J. Comput. Chem.* **1985**, *11*, 431–439.
- (19) Sugihara, M.; Buss, V.; Entel, P.; Elstner, M.; Frauenheim, T. *Biochemistry* **2002**, *41*, 15259–15266.
- (20) The value of the charge transfer, $\Delta\mu$, or f can be taken equivalently as a measure of the ionic character of the wave function. See the Supporting Information.
- (21) Vreven, T.; MoroKuma, K. *Theor. Chem. Acc.* **2003**, *109*, 125–132.
- (22) Zhong, Q.; Ruhman, S.; Ottolenghi, M. *J. Am. Chem. Soc.* **1996**, *118*, 12828–12829.

JA035087D